Acta Pharmacologica Sinica

www.nature.com/aps

ARTICLE

Pharmacokinetics, mass balance, and metabolism of [^{14}C]vicagrel, a novel irreversible P2Y$_{12}$ inhibitor in humans

Yuan-dong Zheng[1,2], Hua Zhang[3,4], Yan Zhan[1,2], Yi-cong Bian[3,4], Sheng Ma[3,4], Hai-xian Gan[1], Xiao-juan Lai[5], Yong-qiang Liu[5], Yan-chun Gong[5], Xue-fang Liu[5], Hong-bin Sun[6], Yong-guo Li[7], Da-fang Zhong[1,2], Li-yan Miao[3,4] and Xing-xing Diao[1,2]

Vicagrel, a novel irreversible P2Y$_{12}$ receptor inhibitor, is undergoing phase III trials for the treatment of acute coronary syndromes in China. In this study, we evaluated the pharmacokinetics, mass balance, and metabolism of vicagrel in six healthy male Chinese subjects after a single oral dose of 20 mg [^{14}C]vicagrel (120 μCi). Vicagrel absorption was fast (T_{max} = 0.625 h), and the mean $t_{1/2}$ of vicagrel-related components was ~38.0 h in both plasma and blood. The blood-to-plasma radioactivity AUC_{inf} ratio was 0.55, suggesting preferential distribution of drug-related material in plasma. At 168 h after oral administration, the mean cumulative excreted radioactivity was 96.71% of the dose, including 68.03% in urine and 28.67% in feces. A total of 22 metabolites were identified, and the parent vicagrel was not detected in plasma, urine, or feces. The most important metabolic spot of vicagrel was on the thiophene ring. In plasma pretreated with the derivatization reagent, M9-2, which is a methylated metabolite after thiophene ring opening, was the predominant drug-related component, accounting for 39.43% of the radioactivity in pooled $AUC_{0-8\,h}$ plasma. M4, a mono-oxidation metabolite upon ring-opening, was the most abundant metabolite in urine, accounting for 16.25% of the dose, followed by M3-1, accounting for 12.59% of the dose. By comparison, M21 was the major metabolite in feces, accounting for 6.81% of the dose. Overall, renal elimination plays a crucial role in vicagrel disposition, and the thiophene ring is the predominant metabolic site.

Keywords: vicagrel; [^{14}C]vicagrel; vicagrel pharmacokinetics; vicagrel metabolism; mass balance; P2Y$_{12}$ receptor inhibitor

Acta Pharmacologica Sinica (2021) 42:1535–1546; https://doi.org/10.1038/s41401-020-00547-7

INTRODUCTION

As currently available irreversible P2Y$_{12}$ receptor inhibitors, thienopyridine antiplatelet agents are widely used for the treatment of myocardial infarction, cerebral infarction, and arterial or venous thrombosis, as well as diseases related to platelet aggregation [1–3]. The thienopyridine P2Y$_{12}$ receptor inhibitors used in clinical settings are clopidogrel and prasugrel [4–6].

However, the use of clopidogrel as a first-line P2Y$_{12}$ receptor inhibitor has a certain disadvantage known as "clopidogrel resistance", in which some patients show low response, no response, or resistance to treatment for cardiovascular diseases [7]. The United States Food and Drug Administration issued a black box warning cautioning that CYP2C19 poor metabolizers are at a higher risk of treatment failure with clopidogrel [8, 9]. Moreover, a high oral dose of clopidogrel is required because it is inefficiently metabolized into active metabolite in vivo. Clopidogrel undergoes a two-step CYP450-dependent oxidation to form the active thiol metabolite in the liver. However, during the process, ~85% of clopidogrel is hydrolyzed by human carboxylesterase 1 to form inactive clopidogrel carboxylic acid, and <15% of clopidogrel is transformed into 2-oxo-clopidogrel in the first step (Fig. 1) [10–12]. The active metabolite M15-2 is generated from 2-oxo-clopidogrel, and the inefficient biotransformation to 2-oxo-clopidogrel in the first step restricts the use of clopidogrel.

Prasugrel, another P2Y$_{12}$ receptor inhibitor commonly used in clinical settings, shows more consistent platelet inhibition and higher efficiency in producing active metabolite than clopidogrel; however, its use leads to a higher risk of bleeding than clopidogrel [13, 14]. Therefore, new thienopyridine antiplatelet agents must be developed to improve the current antiplatelet therapy.

Vicagrel, a novel thienopydine P2Y$_{12}$ antagonist, is undergoing phase III trials in China [9]. Vicagrel, which has a structure similar to that of clopidogrel, also requires a two-step metabolic process to form an active metabolite, and the second step of both agents is exactly the same [15, 16]. In the first step, almost all vicagrel is hydrolyzed by human carboxylesterase 2 and arylacetamide deacetylase to form 2-oxo-clopidogrel [15, 17]; hence, the exposure of 2-oxo-clopidogrel to the two drugs is substantially different (Fig. 1). Thus, a considerably lower dose of vicagrel may yield a plasma exposure of the active metabolite M15-2 comparable to that of clopidogrel. Previous studies demonstrated that the same exposure level of M15-2 can be achieved after oral

[1]State Key Laboratory of Drug Research, Shanghai Institute of Materia Medica, Chinese Academy of Sciences, Shanghai 201210, China; [2]University of Chinese Academy of Sciences, Beijing 100049, China; [3]Department of Clinical Pharmacology, the First Affiliated Hospital of Soochow University, Suzhou 215123, China; [4]Institute for Interdisciplinary Drug Research and Translational Sciences, Soochow University, Suzhou 215006, China; [5]Jiangsu Vcare PharmaTech Co. Ltd., Nanjing 211800, China; [6]State Key Laboratory of Natural Medicines and Center of Drug Discovery, College of Pharmacy, China Pharmaceutical University, Nanjing 210009, China and [7]Guangzhou JOYO Pharma Ltd., Shanghai 201203, China

Correspondence: Da-fang Zhong (dfzhong@simm.ac.cn) or Li-yan Miao (miaolysuzhou@163.com) or Xing-xing Diao (xxdiao@simm.ac.cn)

These authors contributed equally: Yuan-dong Zheng, Hua Zhang

Received: 23 June 2020 Accepted: 23 September 2020
Published online: 26 November 2020

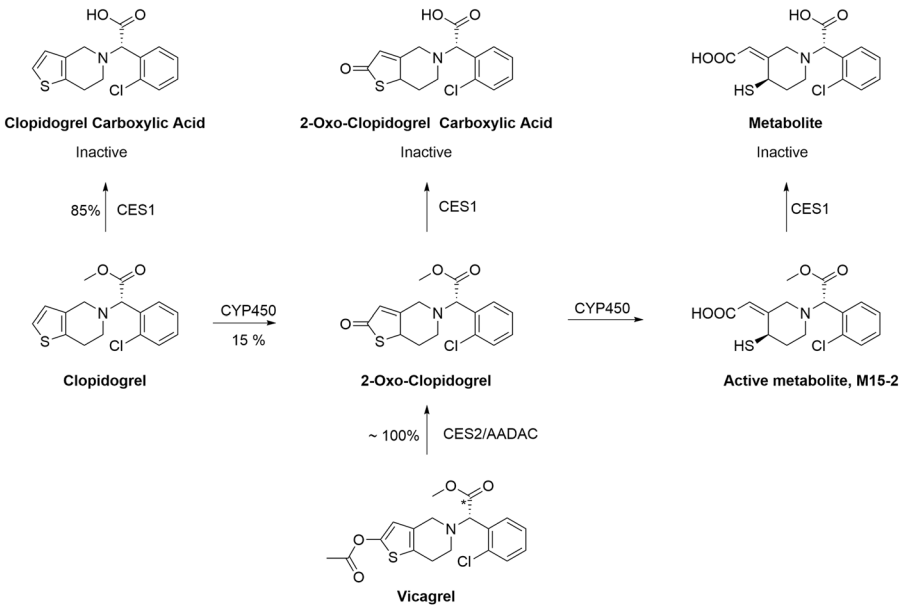

Fig. 1 Main pathway in forming active metabolite of clopidogrel and vicagrel (* indicates ^{14}C labeled position). AADAC arylacetamide deacetylase, CES carboxylesterase.

administration of 5 mg vicagrel versus 75 mg clopidogrel, a finding that is consistent with the proposed drug design hypothesis [18]. In view of these advantages, vicagrel is expected to induce less drug resistance than clopidogrel, as well as to improve drug safety by decreasing the risk of bleeding.

Although vicagrel shows potential as a first-line medicine and has been investigated in numerous studies, its use still has issues [7, 8]. Thus far, no data are available to evaluate its overall in vivo metabolism. Preliminary vicagrel mass balance studies using nonradiolabeled vicagrel demonstrated that ~18% of the dose is excreted, mainly in human urine (unpublished data). However, the fate of the remaining metabolites is still unclear. Owing to the low recovery rate, determining the major metabolites and the metabolism mechanism is difficult. In addition, no data are available concerning the metabolism of [^{14}C]vicagrel in animals or humans. A better understanding of vicagrel metabolism is important to identify its metabolic profile, assess the safety of its metabolites, understand its pharmacokinetics, and determine its mechanisms of clearance, which in turn are necessary to identify potential drug–drug interactions (DDIs) [19–21]. This information is necessary in guiding future clinical evaluations of vicagrel and ultimately determining appropriate dosages for patients [22]. The use of radioactive tracers, such as ^{14}C-labeled compounds, in absorption, distribution, metabolism, and excretion studies enables the determination of the mass balance and major metabolic routes of a drug candidate [23–27]. In the present study, [^{14}C]vicagrel suspension solution was administered to healthy male Chinese subjects, and its pharmacokinetics, mass balance, and biotransformation pathway were investigated.

MATERIALS AND METHODS

Chemical and reagents

Vicagrel (99.20% purity) and the reference substances M3, M6, d_6-M6, M9-2, MP-M15-1, and MP-M15-2 were kindly supplied by Jiangsu Vcare PharmaTech Co., Ltd. (Nanjing, China). Both [^{14}C]vicagrel (120 μCi, 98.68% purity) and vicagrel (20 mg) were dissolved in a 95% ethanol solution (~3 mL, pharmaceutical grade) and preserved at ~–80 °C. The oral suspension was prepared by diluting the ethanol solution with 80 mL pure water on the day of administration. The ^{14}C-label was located on the ester carbonyl group (Fig. 1). The derivatization reagent 2-bromo-3′-methoxyacetophenone (MPB) and high-performance liquid chromatography (HPLC)-grade acetonitrile and methanol were purchased from Sigma (St. Louis, MO, USA). Ammonium acetate was obtained from Sinopharm Chemical Reagent Co., Ltd. (Shanghai, China). Formic acid was purchased from Rhawn Chemical Reagent Co., Ltd. (Shanghai, China). Ultrapure water was obtained from a Milli-Q integral water purification system (Millipore, Molsheim, France). The other commercially available reagents used herein were of analytical grade.

Instruments and conditions

With the help of mass defect filters and background subtraction techniques, high-resolution mass spectrometry (HR-MS) and HR-MS^2 acquisition are widely used for metabolite identification [28, 29]. In the present study, HR-MS and HR-MS^2 acquisition were performed on a Vanquish ultra-high-performance liquid chromatography (UHPLC) system coupled with a Q Exactive Plus mass spectrometer (Thermo, Waltham, MA, USA) equipped with an electrospray ionization (ESI) source. Chromatographic separation was achieved on an Agilent Extend C_{18} column (150 mm × 4.6 mm, 5 μm; Agilent, Santa Clara, CA, USA) at 25 °C with a flow rate of 0.6 mL/min. The mobile phase consisted of 5 mM ammonium acetate in water with 0.05% formic acid (A) and acetonitrile (B). The gradient elution program was as follows: 0 min, 5% B; 3 min, 5% B; 35 min, 35% B; 45 min, 75% B; 46 min, 95% B; 48 min, 95% B; 49 min, 5% B; 60 min, 5% B. The eluent was monitored by UV detection at 254 nm, and (+)ESI mode was applied in MS detection at a scan range of *m/z* 100–800 Da. The optimized MS parameters were as follows: sheath gas, 45 L/min; aux gas, 10 L/min; capillary temperature, 320 °C; aux gas heater temperature, 400 °C; capillary voltage, 3.5 kV. Data acquisition was performed via Xcalibur software (Thermo), and data analysis was accomplished using Compound Discoverer software (Thermo).

Study design, subjects, and sample collection

This open-label, single-center, and single-dose study was conducted at the First Affiliated Hospital of Soochow University (Suzhou, China). Six healthy male Chinese subjects aged between

19 and 36 years with a body mass index between 21 and 26 kg/m^2 were recruited. The study was conducted in compliance with the ethical principles required in the Declaration of Helsinki and approved by the Hospital Ethics Committee. All participants provided written informed consent prior to the commencement of the study. Plasma, urine, and feces samples were collected 0–168 h after oral administration, and the subjects were discharged from the clinic when the following criteria were satisfied: the accumulated excreted radioactivity was over 80% of the administered radioactivity, the excreted radioactivity was lower than 1% of the administered radioactivity over 2 consecutive days, and the measured radioactivity in plasma collected was less than twofold that of predose over 2 consecutive days [30]. The subjects were instructed to stay in the clinical facility for follow-up until they reached normal health conditions if they had major clinically abnormal conditions. Each of the six subjects received a single oral dose of 20 mg [^{14}C]vicagrel (120 μCi) as a suspension solution after fasting for at least 10 h. The bottle used for drug administration was rinsed with pure water, and the volunteers consumed the rinsing fluids (the total volume was ~240 mL) within 5 min. The subjects were prohibited from drinking water for 1 h and fasted for 4 h. Subsequently, 18 mL of whole blood was collected at predose and 0.25, 0.5, 1, 2, 4, 8, and 24 h postdose. From these samples, 7 mL was immediately mixed with esterase inhibitor in an ice water bath, and another 7 mL was immediately mixed with MPB and allowed to react for at least 10 min before centrifugation to yield the respective plasma. Approximately 1 mL of the remaining blood was aliquoted into a blood tube, and the leftover blood (3 mL) was centrifuged to yield plasma. Furthermore, 8 mL of whole blood was collected at 1.5, 2.5, 3, 6, 12, 36, 48, 72, 96, 144, and 168 h. Approximately 2 mL of whole blood was immediately mixed with esterase inhibitor in an ice water bath, and another 2 mL was immediately mixed with MPB and allowed to react for at least 10 min before centrifugation to yield the respective plasma. Approximately 1 mL of the remaining blood was aliquoted into a blood tube, and the leftover blood (3 mL) was centrifuged to yield plasma. Urine samples were collected at predose and 0–4, 4–8, 8–12, 12–24, 24–48, 48–72, 72–96, 96–120, 120–144, and 144–168 h postdose. Fecal samples were collected at predose and 0–24, 24–48, 48–72, 72–96, 96–120, 120–144, and 144–168 h postdose. All samples were preserved at ~−80 °C until analysis.

Safety assessment

Drug safety was evaluated via physical examination, assessment of vital signs, and laboratory tests, and the occurrence of any adverse event was recorded. The vital signs of the subjects were assessed at least once during each study day. Physical examinations were performed before and after each study period. Adverse events were recorded throughout the study period.

Analysis of total radioactivity

The total radioactivity in plasma and urine was measured using a liquid scintillation counter (LSC) (Tri-Carb 3110 TR, Perkin Elmer, Waltham, MA, USA). Each fecal sample was mixed with twice the weight of ethanol-water (1:1, *v*:*v*) and then homogenized. Blood and fecal homogenates were weighed and combusted using an OX-501 Biological Oxidizer (Harvey, Tappan, NY, USA). The $^{14}CO_2$ generated was then trapped in alkaline RDC liquid scintillation cocktail (RDC, Hilladale, NJ, USA) and measured using LSC.

Sample preparation and metabolic radioprofiling

Plasma. The 0–8 h plasma pretreated with MPB from the six subjects was individually pooled according to the Hamilton pooling principle, and then an equal volume from each subject was pooled [31]. An aliquot of pooled plasma sample (4.5 mL) was extracted by adding 13.5 mL methanol-acetonitrile (50:50, *v*:*v*). The mixture was then vortexed for 1 min and centrifuged at 5000 rpm for 10 min at room temperature. The supernatant was transferred into another clean tube, and then the postextraction solid was added to 2.25 mL water and extracted again with 13.5 mL methanol-acetonitrile (50:50, *v*:*v*). The two supernatants were combined and dried under nitrogen at 25 °C. The residues were reconstituted in 400 μL acetonitrile-water (20:80, *v*:*v*), 90 μl of which was injected into the UHPLC-Fraction collector system (Thermo). The UHPLC eluent was collected in Deepwell LumaPlate 96 plates (Perkin Elmer, USA) for 0–48 min with every 8 s eluent collected in one well. The plates were dried at room temperature, and the CPM values were read by a Sense Beta plate reader (Hidex, Turku, Finland). Data were reconstructed into a radiochromatogram by using Laura software (Lablogic, Broomhill, Sheffield, UK). Another 15 μl of the reconstituted solution was injected for UHPLC-Q Exactive Plus MS analysis.

Urine. An equal percentage by volume of each urine sample was pooled for 0–24 h across the six subjects. Then, 9 mL of the pooled urine sample was dried under nitrogen at 25 °C. The residues were reconstituted in 700 μL acetonitrile-water (20:80, *v*:*v*), 35 μL of which was injected for UHPLC-β-RAM (Lablogic, UK) online radioactivity detection. Another 7 μL of the reconstituted solution was injected for UHPLC-Q Exactive Plus MS analysis.

Feces. An equal percentage by weight of each fecal homogenate sample was pooled for 0–48 h across the six subjects. An aliquot of pooled fecal homogenate (5 g) was extracted by adding 15 g methanol-acetonitrile (50:50, *v*:*v*). The mixture was then vortexed for 1 min and centrifuged at 5000 rpm for 10 min at room temperature. The supernatant was transferred into another clean tube, and then the postextraction solid was added to 2.5 mL water and extracted again with 15 g methanol-acetonitrile (50:50, *v*:*v*). The two supernatants were combined and dried under nitrogen at 25 °C. The residues were reconstituted in 550 μL acetonitrile-water (20:80, *v*:*v*), and 35 μL of the reconstituted solution was used for radiochromatogram analysis following the same method applied in plasma samples. Another 15 μL of the reconstituted solution was injected for UHPLC-Q Exactive Plus MS analysis.

Metabolite identification

The structures of metabolites were identified by UHPLC-Q Exactive Plus MS by comparing their mass spectral fragmentations with those produced by the parent compound and other reference substances available. The chlorine isotopic distribution pattern (ratio of 3:1) was also used for metabolite identification.

Determination of M3, M9-2, M15-1, and M15-2 in human plasma

The plasma sample pretreated with esterase inhibitor was used to determine the M3 concentration. The analyte M3 and the internal standard (d_6-M6) were separated on a BEH C_{18} column (50 mm × 2.1 mm, 1.7 μm; Waters, Milford, MA, USA). The column temperature was maintained at 45 °C. The mobile phase consisted of water with 0.05% formic acid and acetonitrile at a flow rate of 0.55 mL/min. Detection was performed in (+)ESI mode by using Qtrap 5500 LC-MS/MS (Sciex, Framingham, MA, USA). The quantitative transition ion pairs were *m/z* 324.0 → 112.9 (M3) and *m/z* 348.2 → 159.0 (d_6-M6).

The plasma sample pretreated with MPB was analyzed to quantify M9-2, M15-1, and M15-2 by using a validated LC-MS/MS method [18, 32].

Pharmacokinetic analysis

Plasma concentration-time data for vicagrel and its metabolites and the total radioactivity concentration-time data for [^{14}C]vicagrel-related components in plasma and blood were analyzed using noncompartmental methods in Phoenix WinNonlin (version 7.0; Pharsight Corporation, Mountain View, CA, USA). The following parameters were calculated: area under the curve (AUC) for plasma concentration versus time up to the last

measurable time point (AUC_{last}), AUC curve to infinity (AUC_{inf}), maximum plasma concentration (C_{max}), time to reach C_{max} (T_{max}), and half-life ($t_{1/2}$). The AUC_{inf} and $t_{1/2}$ values were not calculated unless at least three time points (of which the first time point must be greater than T_{max}) with quantifiable concentrations were obtained. The blood-to-plasma AUC_{inf} ratio was calculated by dividing the AUC_{inf} of total radioactivity in blood by the AUC_{inf} of total radioactivity in plasma. The AUC ratio of metabolites to total radioactivity was calculated by dividing the AUC_{inf} of metabolites by the AUC_{inf} of total radioactivity. The excretion of radioactivity in urine and feces (percentage of dose) was calculated by dividing the excreted radioactivity by the administered radioactivity.

RESULTS

Safety assessment

During the clinical trial, two cases of adverse events occurred in one of six subjects; i.e., the patient experienced bleeding under the left foot nail and fever. Fever was considered to be possibly related to the study drug, and adverse events were recorded and followed up until recovery/cure. The other case (bleeding under the left foot nail) was regarded as possibly unrelated to the study drug. No serious adverse events were reported. According to the Common Terminology Criteria for Adverse Events v. 5.0, the severity of these two adverse events was defined as grade I. Therefore, vicagrel was considered safe in clinical practice.

HR-MS analysis of vicagrel and reference standards of five possible metabolites

The chromatographic and HR-MS fragmentation patterns of vicagrel and five possible metabolic reference standards were examined. The fragmentation patterns of the major product ions were characterized on the basis of accurate mass measurements and used to determine potential metabolites.

Vicagrel, $C_{18}H_{18}O_4NClS$, with $[M+H]^+$ at *m/z* 380.0717, eluted at 47.88 min and showed product ions at *m/z* 152.0260, 184.0521, 212.0469, and 338.0608 (Fig. 2a, b). The base peak ion at *m/z* 212.0469 was generated by N-C cleavage; further neutral loss of CO and a $C_2H_4O_2$ chain led to *m/z* 184.0521 and 152.0260, respectively.

M3, a pair of isomers, possessed protonated ions at *m/z* 324.0458 and 324.0459 with retention times of 19.54 and 20.61 min, respectively. They yielded almost the same product ions at *m/z* 141.0100, 156.0477, 169.0051, and 278.0402 (Fig. 2c, d). M3 was generated from vicagrel by ester hydrolysis at two sites.

M6, also a mixture of isomers, eluted at 21.30 and 21.50 min and displayed the protonated molecular ion *m/z* 342.1107. M6 produced characteristic product ions at *m/z* 141.0783, 155.0258, 183.0206, 282.0889, and 324.0992 (Fig. 2e, f).

M9-2 with $[M+H]^+$ at *m/z* 370.0874 eluted at 41.66 min and showed product ions at *m/z* 155.0258, 183.0205, 212.0470, and 322.0836 (Fig. 2g, h). The ion at *m/z* 322.0836 was generated from neutral loss of CH_3SH and further loss of hydrogen. The other product ions were the same as those of M6.

MP-M15-1 and MP-M15-2 displayed protonated ions at *m/z* 504.1251 and 504.1250 with retention times of 44.92 and 45.42 min, respectively. They yielded similar product ions at *m/z* 155.0259, 183.0207, 212.0471, and 354.0558 (Fig. 2i, j). The product ion at *m/z* 354.0558 was generated by cleavage of MPB and further loss of hydrogen. The other product ions were similar to those of M9-2.

Pharmacokinetics

The radioactivity concentration-time profiles in blood and plasma after a single oral administration of 20 mg [^{14}C]vicagrel (120 μCi) to healthy male Chinese subjects are shown in Fig. 3a, and the related pharmacokinetic parameters for radioactivity are summarized in Table 1. In plasma and blood, the mean C_{max} values of radioactivity were 1430 and 694 ng eq./mL, the mean AUC_{last} values were 11,200 and 6020 ng eq./mL·h, and the mean AUC_{inf} values were 13,700 and 7590 ng eq./mL·h, respectively. The mean T_{max} and $t_{1/2}$ were ~0.625 and 38 h in blood and plasma, respectively. The blood-to-plasma AUC_{inf} ratio of the radioactivity was 0.55. The mean plasma concentrations of the metabolites are shown in Fig. 3b. The pharmacokinetic parameters of vicagrel and its metabolites are presented in Table 1. The mean T_{max} of M3, M9-2, M15-1, and M15-2 was 0.42, 0.83, 0.42, and 0.33 h, respectively. The mean $t_{1/2}$ of M3, M9-2, M15-1, and M15-2 was 1.97, 13.40, 2.54, and 2.05 h, respectively. The mean C_{max} of M3 was 405, 288, 76.4 and 60.1 ng/mL, respectively. The mean exposure (AUC_{inf}) of M9-2, M3, M15-1, and M15-2 was 2890, 461, 59.0, and 41.8 ng/mL·h, respectively. According to the AUC_{inf} total radioactivity ratios, M9-2 was the most abundant moiety in plasma (21.09%), followed by M3 (3.36%), M15-1 (0.43%), and M15-2 (0.31%).

Mass balance

In the six healthy male Chinese subjects after oral administration of 20 mg [^{14}C]vicagrel (120 μCi), the mean total radioactivity recovery was 96.71% (93.14%–100.90%). Urine excretion was the predominant route of elimination, accounting for a mean of 68.03% of the administered dose, whereas the mean fecal excretion was 28.67%. The total recovery of radioactivity in urine and feces at 48 and 72 h after dosing was 92.00% and 94.41%, respectively, as shown in Fig. 3c.

Quantitative metabolite profiling

The UHPLC eluents of 0–8 h plasma and 0–48 h fecal samples were collected by a UHPLC-Fraction collector into Deepwell LumaPlate 96 plates. The radioactivity in each well was counted by Sense Beta and then used to reconstruct the respective radiochromatograms by using Laura software. The 0–24 h urine sample was injected for UHPLC separation, followed by β-RAM online radio-detection. Plasma, urine, and fecal samples were also injected for UHPLC-Q Exactive Plus MS analysis.

The radiochromatograms of 0–8 h plasma, 0–24 h urine, and 0–48 h fecal samples are shown in Fig. 4. The identities of 22 proposed metabolites, including their biotransformation, elemental composition, protonated *m/z* ($[M+H]^+$) values, mass error (ppm), and characteristic fragment ions, are summarized in Table 2. The nomenclature of the metabolites is consistent with that from Dr. Cai Liu's doctoral dissertation for the already identified metabolites; for the newly identified metabolites, the assigned name was the molecular weight prefixed with "M".

Plasma. In AUC-pooled 0–8 h plasma, unchanged vicagrel was not detected, and a total of 12 radiochromatographic peaks were identified (Fig. 4). Among them, M9-2 was the predominant drug-related component in the AUC-pooled 0–8 h plasma pretreated with MPB. This result was consistent with that of a previous study [18].

M9-2. The protonated molecular ion $[M+H]^+$ of M9-2 was detected at *m/z* 370.0879 with a formula of $C_{17}H_{20}O_4NClS$ according to exact mass measurement. The major product ions of M9-2 were at *m/z* 155.0258, 183.0205, 212.0469, and 322.0836 (Fig. 5a, b). The structure of M9-2 was confirmed by comparing the retention time and LC-MS/MS spectrum with those of the reference standard.

Several metabolites (M3-1, M4, M8, M352, M11-4, MP-M15-1, and MP-M15-2) were identified as minor metabolites of vicagrel. The structures of MP-M15-1 and MP-M15-2 were confirmed by comparing them with reference standards. M9-2, M3-1, M8, M352, and M4 accounted for 39.43%, 8.71%, 5.70%, 5.23%, and 3.48% of the total plasma radioactivity, respectively.

Urine. In the 0–24 h pooled urine sample, a total of 13 radiochromatographic peaks were identified, but the parent

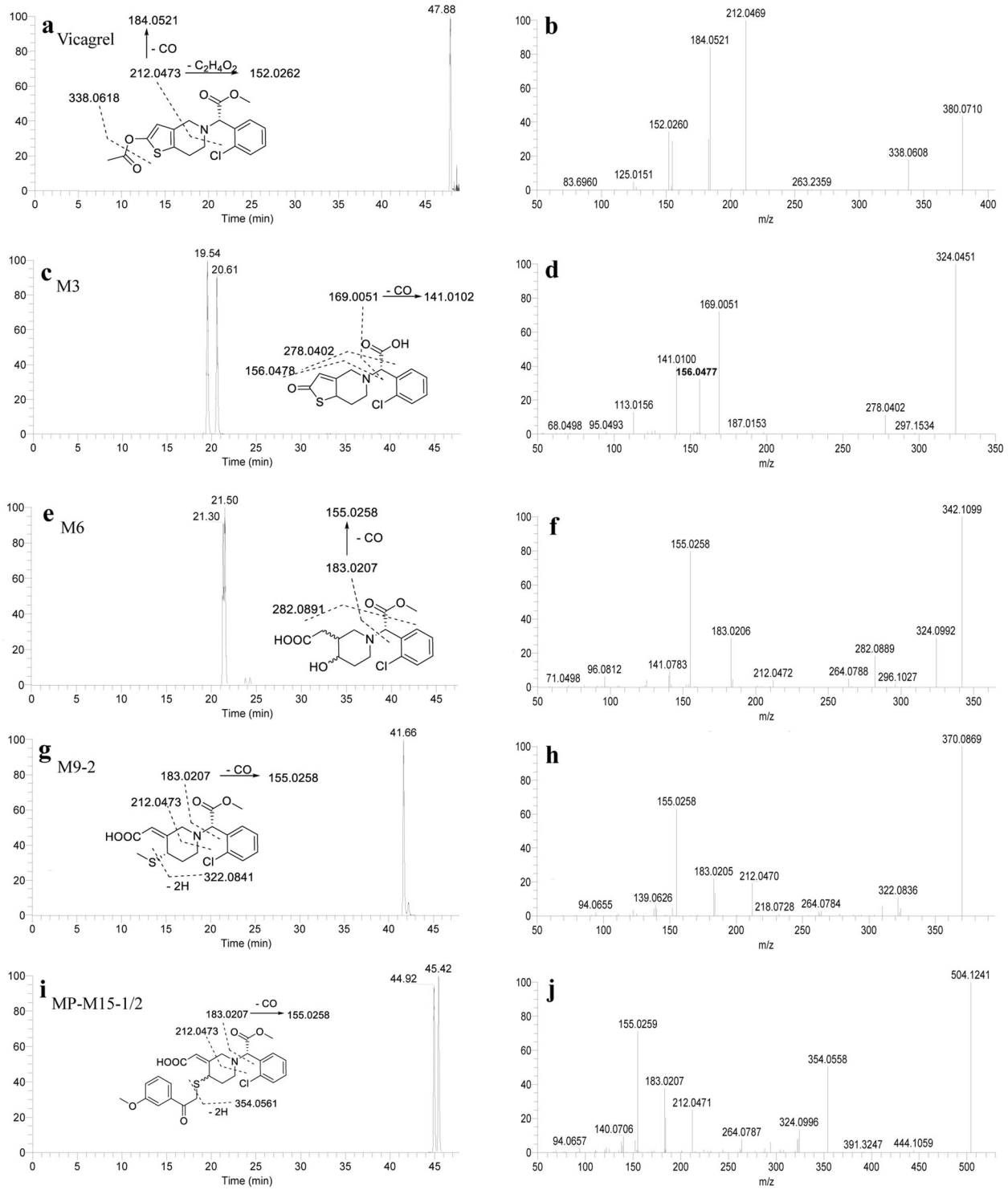

Fig. 2 Extracted ion chromatograms, product ion spectra, and proposed fragmentaion patterns. Vicagrel (**a**, **b**), M3 (**c**, **d**), M6 (**e**, **f**), M9-2 (**g**, **h**), MP-M15-1/MP-M15 (**i**, **j**).

vicagrel was not detected (Fig. 4). Four abundant metabolites were assigned as M3-1, M4, and M5/M2 (coeluting), accounting for 12.59%, 16.25%, and 11.28% of the dose, respectively.

M3-1. The $[M + H]^+$ of M3-1, *m/z* 324.0459, was 56.0261 Da lower than that of vicagrel and possessed the same molecular weight as the reference standard M3. The formula obtained from exact mass measurement implied the loss of C_3H_4O, corresponding to the loss of CH_2CO (42.0106 Da) and CH_2 (14.0157 Da) from the parent drug. The main ions at *m/z* 141.0101, 152.0260, 169.0051, and 198.0314 also supported the structure of M3-1 (Fig. 5c, d). The double bond position was proposed by comparing the LC-MS/MS spectrum with that of the reference substance of M3.

M4. The $[M + H]^+$ of M4, *m/z* 340.0411, was 15.9952 Da larger than that of M3. The calculated elemental composition was

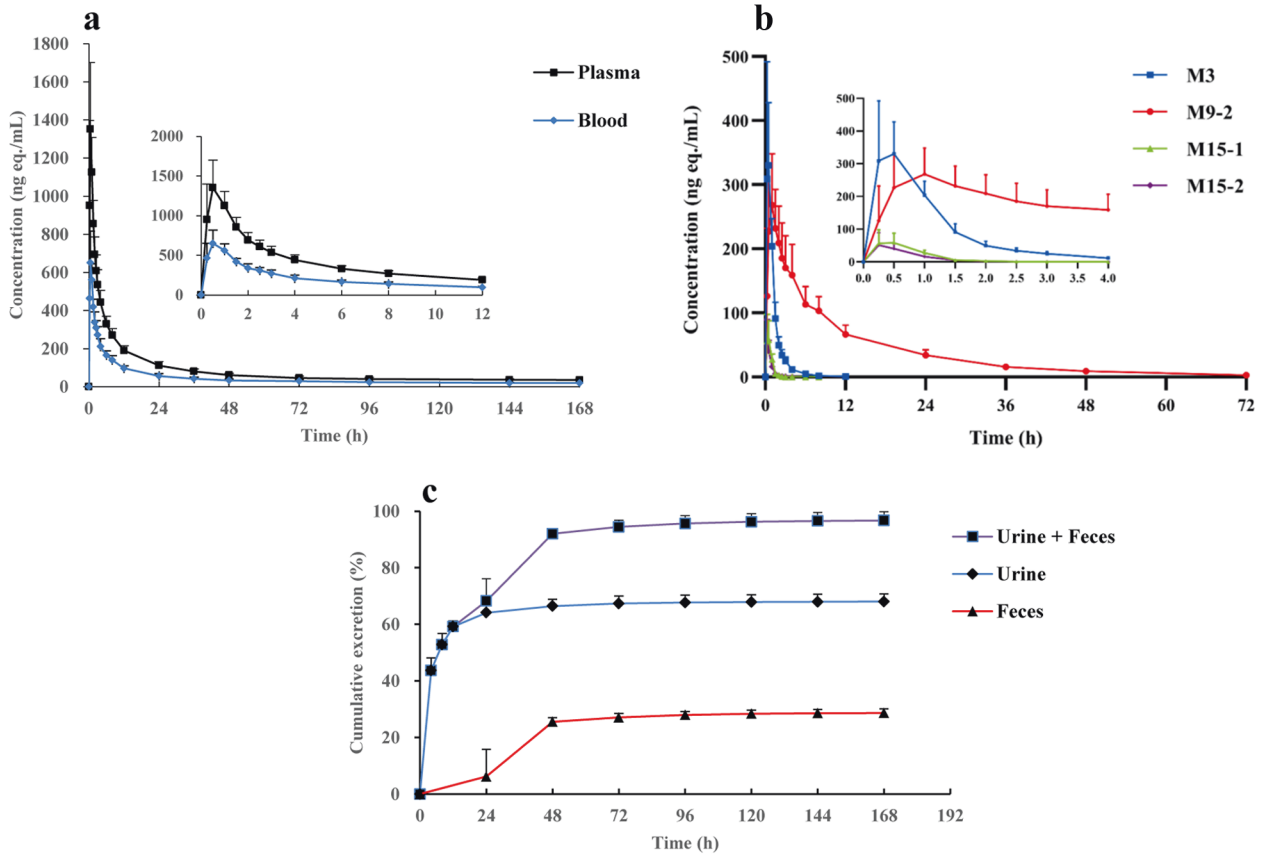

Fig. 3 Radioactive pharmacokinetics, LC-MS/MS analysis, Mass balance. (**a**), mean concentration of radioactivity in blood and plasma; (**b**), mean concentration of metabolites M3, M9-2, M15-1 and (**c**), M15-2 in plasma and mean cumulative excretion of total radioactivity in urine and feces following a single oral administration of [14C]vicagrel . Each point represents the mean ± SD of six subjects.

$C_{15}H_{14}O_4NClS$, indicating mono-oxidation of M3. The same product ions at *m/z* 141.0100 and 169.0052 as those of M3 suggested that the oxidation was located at the thienopyridine moiety (Fig. 5e, f). The double bond could not be confirmed by MS data alone.

M5. The $[M + H]^+$ of M5, *m/z* 340.0951, was 2.0163 Da lower than that of M6. The calculated elemental composition was $C_{16}H_{18}O_5NCl$, indicating dehydrogenation of M6. The main ions at *m/z* 139.0627, 155.0258, 183.0206, and 212.0470 supported the structure of M5 (Fig. 5g, h). The stereochemistry of the hydroxyl moiety could not be confirmed by the MS data.

M2. The $[M + H]^+$ of M2, *m/z* 324.1003, was 18.0111 Da lower than that of M6. The calculated elemental composition was $C_{16}H_{18}O_4NCl$, indicating a water molecule less than that of M6. The accurate mass product ions at *m/z* 155.0258, 184.0521, and 212.0470 also supported the structure of M2 (Fig. 5i, j).

Several phase II glucuronide acid conjugates (M14-1, M14-2, M18-1, and M18-2) were also detected as minor metabolites in urine.

Feces. A total of 12 radiochromatographic peaks were identified in the pooled 0–48 h fecal samples (Fig. 4). Among them, two abundant metabolites, M352 and M21, accounted for 6.81% and 4.76% of the dose, respectively.

M352. The $[M + H]^+$ of M352 was detected at *m/z* 353.1269. Its calculated elemental composition was $C_{17}H_{23}O_4N_2Cl$ according to exact mass measurement. The main product ions were at *m/z* 152.0261, 169.0052, 198.0314, 264.0783, and 307.1203. The structure of M352 was deduced by comparing its ion fragments with those of M3 and M6 (Fig. 5k, l).

M21. The $[M + H]^+$ of M21, *m/z* 310.0850, was 14.0153 Da lower than that of M2, implying the loss of CH_2 (14.0157 Da) from M2. Its calculated elemental composition was $C_{15}H_{16}O_4NCl$, indicating that M21 was generated by ester hydrolysis from M2. The accurate mass product ions at *m/z* 152.0261, 169.0051, and 198.0314 also supported the structure of M21 (Fig. 5m, n).

M7-1, M11-4, and M1 were also identified in the fecal sample as minor metabolites.

DISCUSSION

This study reported the pharmacokinetics, mass balance, and metabolism of [^{14}C]vicagrel in humans. The metabolic profile of vicagrel was determined in plasma, urine, and fecal samples after oral administration of 20 mg [^{14}C]vicagrel (120 μCi) suspension solution in six healthy male Chinese subjects. In expected real-world clinical practice after marketing, the recommended regimen is 20 mg as the starting dose and 5 mg as the subsequent maintenance dose. After oral administration, 96.71% of the dosed radioactivity was recovered in urine (68.03%) and feces (28.67%) at 168 h postdose, indicating complete excretion. Mass balance analysis indicated that the predominant route of elimination for drug-related material was renal excretion, a result consistent with that of a previous study (unpublished, Dr. Cai Liu's doctoral dissertation).

On the basis of high radioactivity recovery, metabolite profiling in plasma, urine, and fecal samples was conducted. A total of 22 metabolites were identified, and unchanged vicagrel was not detected in the plasma, urine, or fecal samples following oral administration of [^{14}C]vicagrel. Actually, the result of "the parent compound has not been detected in any matrix" was what we expected. Vicagrel, as a structural analog of clopidogrel, was

Table 1. Pharmacokinetic parameters of radioactivity in blood, plasma, and metabolites in plasma after a single oral administration of [^{14}C]vicagrel to healthy volunteers (mean ± SD) using noncompartmental methods in Phoenix WinNonlin.

Parameter	Unit	^{14}C Plasma	^{14}C Blood	M3	M9-2	M15-1	M15-2
C_{max}	ng eq./mL	1430 (363)	694 (146)	405 (156)	288 (88)	76.4 (40.6)	60.1 (37.0)
AUC_{last}	ng eq./mL·h	11,200 (3350)	6020 (1780)	459 (97)	2840 (682)	58.7 (24.5)	41.5 (14.8)
AUC_{inf}	ng eq./mL·h	13,700 (3500)	7590 (2060)	461 (97)	2890 (686)	59.0 (24.4)	41.8 (14.8)
$t_{1/2}$	h	37.3 (10.0)	38.5 (21.8)	1.97 (0.39)	13.40 (0.71)	2.54 (2.15)	2.05 (0.91)
T_{max}	h	0.625 (0.306)	0.625 (0.306)	0.42 (0.13)	0.83 (0.26)	0.42 (0.13)	0.33 (0.13)

C_{max} and T_{max} were obtained from the quantification data. The area under the plasma concentration versus time curve (AUC_{0-t}) was calculated from 0 to the last measurable time point (t) on the basis of linear trapezoidal approximation. The terminal elimination rate constant (k_e) was evaluated using the log-linear regression of the plasma concentration during the elimination phase. Half-time ($t_{1/2}$) was calculated as $0.693/k_e$. The AUC from 0 to infinity (AUC_{inf}) was estimated as the sum of (AUC_{0-t}) and C_t/k_e, where C_t is the concentration at the last quantified time point.

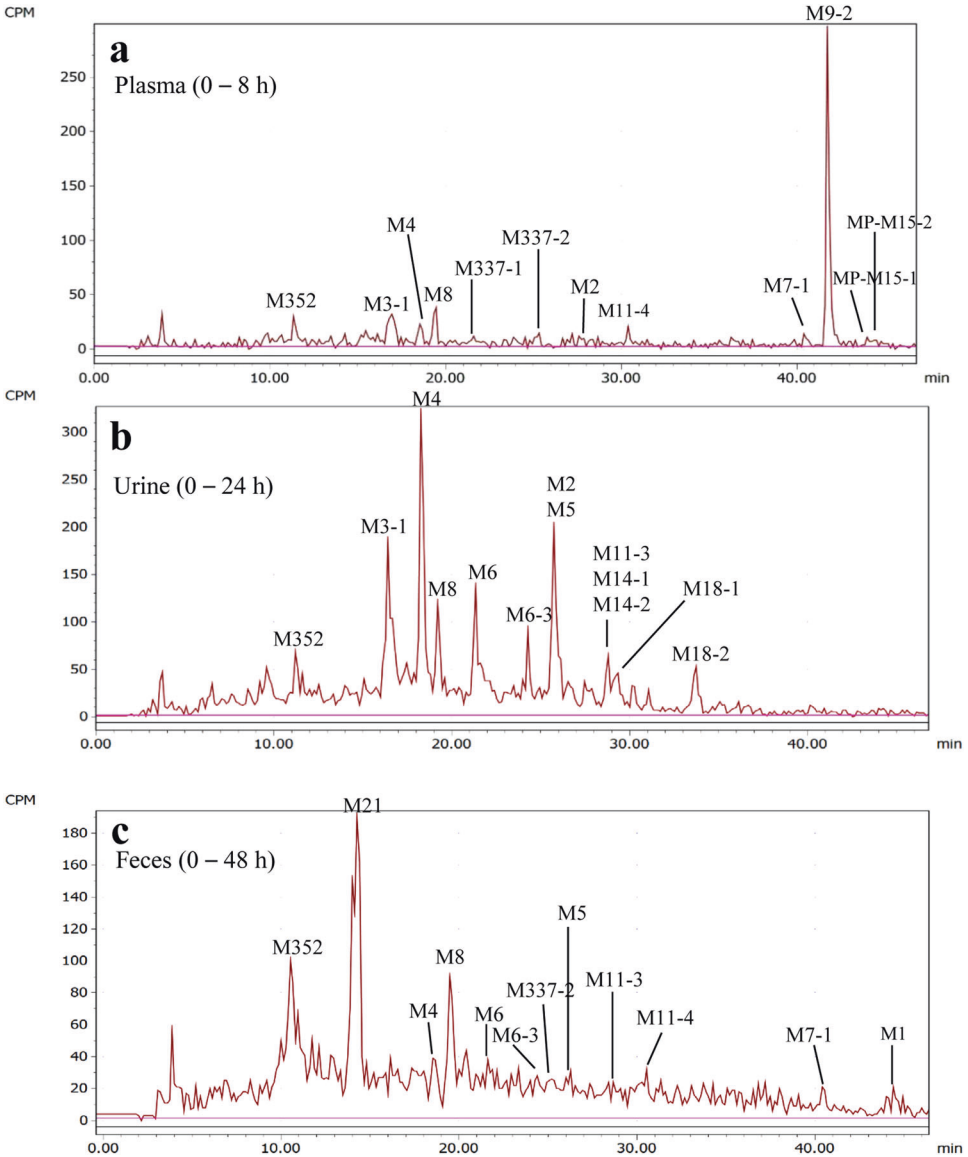

Fig. 4 Representative radio-chromatograms of metabolites. (**a**), Plasma (0–8 h); (**b**), Urine (0–24 h); (**c**), Feces (0–48 h).

Table 2. Information of vicagrel metabolites detected in human plasma, urine, and feces by using UHPLC-Q Exactive Plus MS.

ID	Metabolic pathway	Formula	Retention time (min)	$[M+H]^+$ *m/z* (determined)	Mass error (ppm)	Fragment ions
Vicagrel	Parent	$C_{18}H_{18}O_4NClS$	Not detected	380.0717	−0.3	338.0608, 212.0469, 184.0521, 152.0260
M1	Parent–[A]	$C_{16}H_{16}O_3NClS$	44.27–44.67	338.0614	0.5	278.0.99, 183.0205, 155.0258
M2	M6–H_2O	$C_{16}H_{18}O_4NCl$	25.33–26.40	324.1003	1.7	264.0784, 212.0470, 184.0521, 155.0258
M3-1	Parent–[A]–[M]	$C_{15}H_{14}O_3NClS$	16.00–17.07	324.0459	1.1	198.0314, 169.0051, 152.0260, 141.0101
M337-1	M6–2[2H]	$C_{16}H_{16}O_5NCl$	24.42–24.88	338.0794	1.3	306.0530, 169.0052, 141.0100
M337-2	M6–2[2H]	$C_{16}H_{16}O_5NCl$	25.07–25.73	338.0794	1.4	306.0517, 169.0051, 141.0100
M4	M3 + [O]	$C_{15}H_{14}O_4NClS$	18.27–19.07	340.0411	1.8	322.0295, 169.0052, 141.0100
M5	M15 + [O]–[S]	$C_{16}H_{18}O_5NCl$	25.87–26.40	340.0951	1.3	322.0838, 212.0470, 183.0206, 155.0258, 139.0627
M6	Ring opening + [O]–[S]–[2H]	$C_{16}H_{20}O_5NCl$	21.47–22.00	342.1114	3.3	324.0992, 282.0889, 183.0206, 155.0258, 141.0783
M6-3	Ring opening + [O]–[S]–[2H]	$C_{16}H_{20}O_5NCl$	24.13–24.80	342.1110	2.0	324.0991, 282.0888, 183.0205, 155.0257, 141.0783
M352	M21 + C_2H_5N	$C_{17}H_{23}O_4N_2Cl$	9.87–11.47	353.1269	1.9	307.1203, 264.0783, 198.0314, 169.0051, 152.0261
M7-1	M1 + [O]	$C_{16}H_{16}O_4NClS$	40.27–40.67	354.0569	2.1	336.0451, 294.0350, 276.0244, 183.0206, 155.0258
M8	M9-2–[M]	$C_{16}H_{18}O_4NClS$	19.07–19.87	356.0720	0.7	308.0678, 198.0312, 169.0051, 141.0100
M9-2	Ring opening + [M]	$C_{17}H_{20}O_4NClS$	41.47–43.07	370.0879	1.3	322.0836, 212.0469, 183.0205, 155.0258
M11-3	M9-2 + [O]	$C_{17}H_{20}O_5NClS$	28.40–29.07	386.0822	−0.3	323.0913, 264.0784, 212.0470, 184.0522, 140.0704
M11-4	M9-2 + [O]	$C_{17}H_{20}O_5NClS$	28.00–29.20	386.0829	1.6	323.0915, 264.0783, 212.0468, 184.0524, 140.0704
M14-1	M3 + [GluA]	$C_{21}H_{22}O_9NClS$	28.00–29.20	500.0778	0.2	324.0450, 278.0398, 169.0051, 156.0477
M14-2	M3 + [GluA]	$C_{21}H_{22}O_9NClS$	28.00–29.20	500.0777	0.1	324.0450, 278.0398, 169.0051, 156.0477
MP-M15-1	Ring opening + MPB	$C_{25}H_{26}O_6NClS$	44.00–44.40	504.1251	1.8	354.0558, 324.0996, 212.0471, 183.0207, 155.0259
MP-M15-2	Ring opening + MPB	$C_{25}H_{26}O_6NClS$	44.40–44.90	504.1247	0.9	354.0557, 324.0995, 212.0470, 183.0206, 155.0259
M18-1	M9-2 + [GluA]	$C_{23}H_{28}O_{10}NClS$	29.07–29.47	546.1199	0.8	370.0876, 212.0469, 184.0521, 152.0261
M18-2	M9-2 + [GluA]	$C_{23}H_{28}O_{10}NClS$	33.20–34.27	546.1204	1.7	370.0869, 322.0836, 212.0470, 183.0206, 155.0258
M21	M2–[M]	$C_{15}H_{16}O_4NCl$	13.60–14.76	310.0850	2.9	264.0783, 198.0314, 169.0051, 152.0261

The HR-MS and HR-MS2 acquisition was performed on a Vanquish ultra-high-performance liquid chromatography (UHPLC) system coupled with a Q Exactive Plus mass spectrometer equipped with an electrospray ionization (ESI) source. All possible metabolites were inputted into the inclusion list, and the MS/MS data were acquired when the target *m/z* ions were detected.
[A] acetyl, *[GluA]* glucuronidation, – *[2H]* dehydrogenation, *[M]* methyl, *MPB* 2-bromo-3′-methoxyacetophenone, *[O]* oxidation, *Ring opening* thiophene ring opening, *[S]* sulfur.

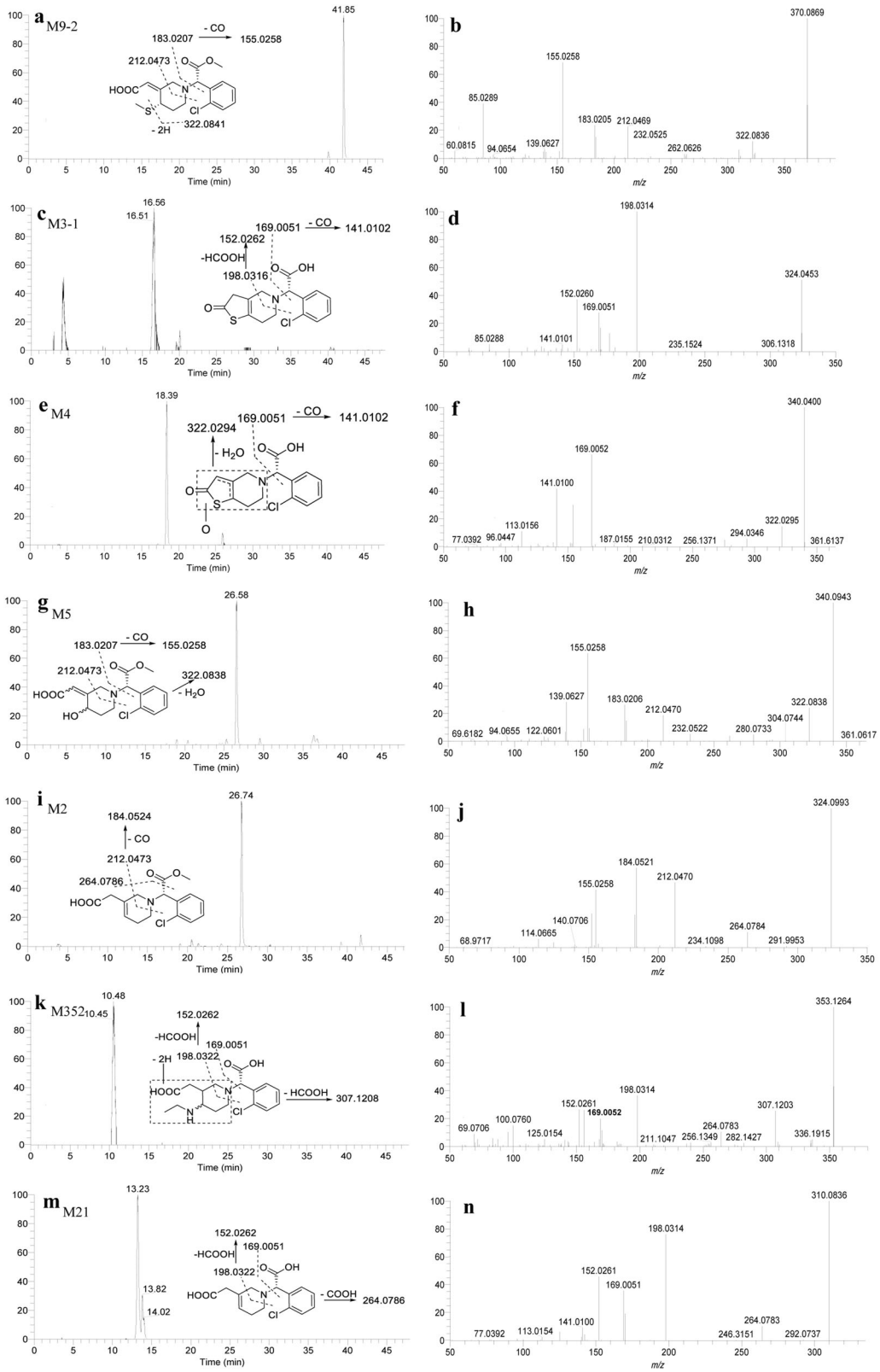

Fig. 5 Extracted ion chromatograms, product ion spectra, and proposed fragmentaion patterns. M9-2 (**a**, **b**), M3-1 (**c**, **d**), M4 (**e**, **f**), M5 (**g**, **h**), M2 (**i**, **j**), M352 (**k**, **l**) and M21 (**m**, **n**).

designed as a prodrug on the basis of clopidogrel metabolism. As shown in Fig. 1, 85% of clopidogrel underwent ester hydrolysis (C-7) to clopidogrel carboxylic acid, which is an inactive metabolite. Only 15% of clopidogrel was oxidized (C-17) to 2-oxo-clopidogrel, the precursor of the active metabolite M15-2. For vicagrel, which possesses a second ester moiety, the ester at C-17 was preferably hydrolyzed rather than the ester at C-7 to form 2-oxo-clopidogrel; hydrolysis efficiency was almost 100%, and thus, no parent drug was

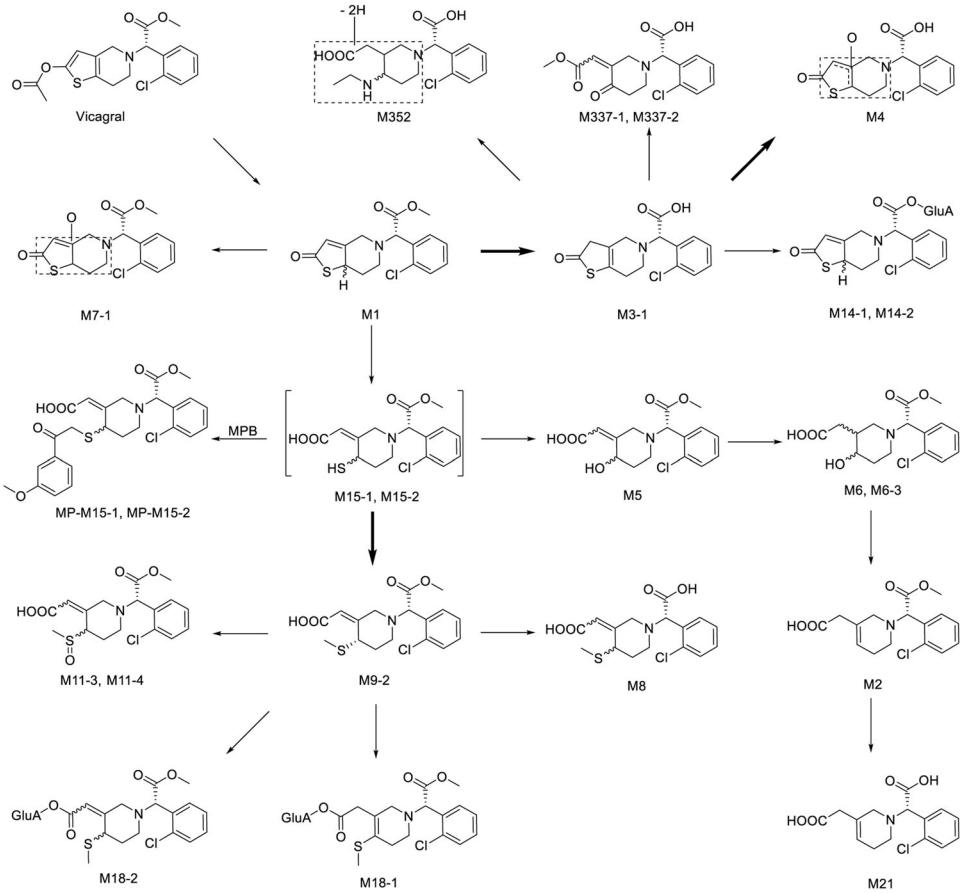

Fig. 6 Metabolic pathway of vicagrel in healthy Chinese male subjects. GluA glucuronic acid, MPB derivation reagent (2-bromo-3′-methoxyacetophenone).

detected in any matrix. The subsequent metabolic pathway from 2-oxo-clopidogrel was the same as that of clopidogrel. As evidence of the success of this drug design hypothesis, the exposure of M9-2 and MP-M15-2 was detected at almost the same concentration in the 5 mg vicagrel dose group and the 75 mg clopidogrel dose group [18].

In plasma pretreated with the derivatization reagent MPB, M9-2 was the predominant drug-related component, accounting for 39.43% of radioactivity in the pooled $AUC_{0-8\,h}$ plasma. The concentration of M9-2, the most abundant metabolite in plasma, was similar to that from previous clinical trials [18]. The concentrations of the other metabolites, such as M3, M15-1, and M15-2, were also at the same level. In urine, M4 was the most abundant metabolite, accounting for 16.25% of the dose, followed by M3-1, accounting for 12.59% of the dose. In feces, M21 was the major metabolite, accounting for 6.81% of the dose.

The biotransformation pathway proposed herein is shown in Fig. 6. Phase I metabolism, such as deacetylation, demethylation, hydrolysis, and reduction, was the major metabolic pathway, whereas phase II metabolism, such as glucuronidation and methylation, was the minor metabolic pathway. As shown in Fig. 6, the most susceptible metabolic site of vicagrel was the thiophene ring, resulting in *S*- or *R*-isomerization at C-4 and *E*- or *Z*-isomerization at the double bond between C-3 and C-16 [33, 34]. Although several reference standards were synthesized to characterize the structures of the metabolites, determining the exact structures of multiple isomers was challenging. On the basis of the MS^2 spectra of available reference standards and possible metabolites, the product ions at *m/z* 212.0470, 198.0314 (212.0470–CH_2), 183.0208, and 169.0051 (183.0208–CH_2) were used as diagnostic ions to determine the position of the double bond. However, this rule is not absolutely applicable and has some exceptions.

Among all metabolites, M352 showed a distinctive structure that has never been reported before. Its calculated elemental composition, $C_{17}H_{23}O_4N_2Cl$, had one more nitrogen atom than the parent drug, indicating that M352 might be generated from a metabolic intermediate through conjugation with amino acids. Alanine, one of the most abundant amino acids in healthy humans, was considered the most likely because of its low molecular weight. The proposed formation mechanism of M352 includes the following two pathways. First, alanine, as a nucleophilic reagent, attacks the mercaptomethyl group at the C-4 position to form a metabolic intermediate in which the alanine is substituted as a new group. The reaction is considered an S_N2 reaction, and during the process, mercaptomethyl is considered a good leaving group [35]. The other possible mechanism is that the ketone in the C-4 position is prone to amination reactions and forms enamine with alanine, which is then transformed to a metabolic intermediate by reductase [36]. Why did we not observe ketones from the metabolic pathway? The metabolites with ketones at the C-4 position tended to form compounds possessing hydroxyl groups, such as M5, M6, and M6-3. Finally, M352 is generated from the metabolic intermediate via decarboxylation [37]. On the basis of this premise, we attempted to isolate M352 to identify its exact structure via nuclear magnetic resonance but failed to obtain a sufficient amount because M352 was a minor metabolite in feces.

According to the 2020 FDA guidance *Safety Testing of Drug Metabolites Guidance for Industry*, metabolites constituting over 10% of the total drug-related exposure in plasma should be

evaluated for safety concerns. In this study, we collected 0–168 h plasma from six subjects and measured the radioactivity for each time point. We also evaluated AUC pooling at 0–12 h or 0–24 h to analyze the metabolite profiles in addition to 0–8 h pooling. However, the concentration in the pooled sample was insufficient for metabolite identification. After balancing the pooling time interval and sample concentration in pooled plasma, we finally chose 0–8 h. In this study, only M9-2 accounted for over 10% of the total drug-related components in human plasma. Several in vitro and in vivo drug metabolism and pharmacokinetics studies were performed in-house or outsourced by Vcare Company. In an in vitro study, the percentages of metabolites detected in human S9 were similar to those in monkey, rat, and dog S9 (unpublished data). In a drug metabolism study after intragastric administration of [^{14}C]vicagrel in rats, no parent compound was detected in plasma, urine, feces or bile. In rat plasma, M9-2 and MP-M15-2 were the major metabolites. The AUC of M9-2 was 2862 ng/mL·h in male rats and 5264 ng/mL·h in female rats after oral administration of 18 mg/kg vicagrel. In the current study, M9-2 exposure in humans (20 mg) was 2840 ng/mL·h. Thus, no further testing was required to evaluate its safety.

A previous study reported that M15-2 is the main active metabolite of vicagrel [38]. M15-2, which possesses a thioenol group, is unstable in vivo. Thus, a derivatization reagent, namely, MPB, was used to pretreat blood to trap M15-2 to MP-M15-2 for further quantitation. However, comparing the AUC of M9-2/MP-M15-1/MP-M15-2 with that of plasma not pretreated with MPB is inaccurate, while we would not obtain any information about the active metabolite M15-2 if we had identified the metabolites in the unpretreated plasma sample. Moreover, the results of the quantitative study and radiochromatograms of M3 showed remarkable differences. In the quantitative study, M3 was found to be a major drug-related component, but it was almost undetectable in the $AUC_{0-8\,h}$ pooled plasma radiochromatogram. The inconsistency was due to different plasma sample types. The plasma sample used for quantitative analysis of M3 was from blood pretreated with esterase inhibitor, whereas that for radiochromatograms was from blood pretreated with MPB rather than esterase inhibitor.

Recently, our laboratory reported the effects of CYP2C19 genetic polymorphisms on vicagrel and clopidogrel [7]. The results demonstrated that CYP2C19 genetic polymorphisms have a considerable effect on clopidogrel in both PK and PD but only a slight influence on vicagrel. We attributed this difference to their different mechanisms in their first step in producing 2-oxo-clopidogrel from clopidogrel or vicagrel. For clopidogrel, the first step is mediated by CYP2C19, whereas carboxylesterase 2 and arylacetamide deacetylase play an important role for vicagrel. Such differences imply that CYP2C19 genetic polymorphisms have a lesser influence on vicagrel than on clopidogrel. The subsequent metabolism from 2-oxo-clopidogrel in vicagrel is the same as that in clopidogrel. Therefore, the possibility of DDI mediated by the CYP2C19 polymorphism in vicagrel is markedly lower than that in clopidogrel. A prior study investigated the DDI between vicagrel and aspirin in rodents [39]. The results showed that vicagrel can increase platelet responses to aspirin and enhance the inhibition of thrombus formation by aspirin, whereas aspirin does not enhance thrombus inhibition by vicagrel.

Vicagrel, as a promising $P2Y_{12}$ receptor inhibitor, addresses clopidogrel resistance in the clinical use of clopidogrel by changing the metabolic pathway as described in this article. The results of preclinical and phase I studies have demonstrated that vicagrel has a definite antiplatelet aggregation effect, rapid onset, and good safety.

In conclusion, this study expands our understanding of the absorption, metabolism, and excretion of vicagrel in humans. Mass balance analysis revealed that 96.71% of the dose was recovered in urine (68.03%) and feces (28.67%) after oral administration. In plasma pretreated with MPB, M9-2 was the predominant drug-related component. M4 and M3-1 were the most abundant metabolites in urine, accounting for 16.25% and 12.59% of the dose, respectively; meanwhile M21 was the major metabolite in feces, accounting for 6.81% of the dose.

ACKNOWLEDGEMENTS

The study was sponsored by Jiangsu Vcare PharmaTech Co., Ltd., and was partially financially supported by a grant from the National Natural Science Foundation of China (No. 81903701). This work was also supported by the National Key New Drug Creation Special Programs (2017ZX09304-021), the Suzhou Key Laboratory of Drug Clinical Research and Personalized Medicine (SZS201719), and the Special Research Fund of Wu Jieping Medical Foundation of Clinical Pharmacy Branch of Chinese Medical Association (320.6750.19090-50).

AUTHOR CONTRIBUTIONS

YDZ, DFZ, YZ, HXG, and XXD were responsible for sample analysis and writing of the manuscript; HZ, YCB, SM, XXD, XJL, and LYM designed the scheme of this clinical study and recruited volunteers; HZ, YCB, and SM were responsible for sample collection in the clinic; XJL, XFL, YGL, YCG, HBS, and YQL offered the test drug and extended financial support.

ADDITIONAL INFORMATION

Competing interests: XJL, XFL, YCG, and YQL are the employees of Jiangsu Vcare PharmaTech Co., Ltd.; and YGL is the consultant of Jiangsu Vcare PharmaTech Co., Ltd. The other authors declare that they have no competing interest.

REFERENCES

1. Gao Y, Yu C, Pi SL, Mao L, Hu B. The role of $P2Y_{12}$ receptor in ischemic stroke of atherosclerotic origin. Cell Mol Life Sci. 2019;76:341–54.
2. Winter MP, Grove EL, Caterina RD, Gorog DA, Ahrens I, Geisler T, et al. Advocating cardiovascular precision medicine with $P2Y_{12}$ receptor inhibitors. Eur Heart J Cardiovasc Pharmacother. 2017;3:221–34.
3. Winter MP, Koziński M, Kubica J, Aradi D, Siller-Matula JM. Personalized antiplatelet therapy with $P2Y_{12}$ receptor inhibitors: benefits and pitfalls. Adv Inter Cardiol. 2015;11:259–80.
4. Cui YM, Wang ZN, Chen XW, Zhang HL, Zhao X, Zhou Y. Pharmacokinetics and pharmacodynamics of single and multiple doses of prasugrel in healthy native Chinese subjects. Acta Pharmacol Sin. 2012;33:1395–400.
5. Amin AM, Chin LS, Noor DAM, Kader MASA, Hay YK, Ibrahim B. The personalization of clopidogrel antiplatelet therapy: the role of integrative pharmacogenetics and pharmacometabolomics. Cardiol Res Pr. 2017;2017:1–17.
6. Jakubowski JA, Matsushima N, Asai F, Naganuma H, Brandt JT, Hirota T, et al. A multiple dose study of prasugrel (CS-747), a novel thienopyridine $P2Y_{12}$ inhibitor, compared with clopidogrel in healthy humans. Br J Clin Pharmacol. 2006;63:421–30.
7. Zhang YF, Zhu XX, Zhan Y, Li XJ, Liu C, Zhu YT, et al. Impacts of CYP2C19 genetic polymorphisms on bioavailability and effect on platelet adhesion of vicagrel, a novel thienopyridine $P2Y_{12}$ inhibitor. Br J Clin Pharmacol. 2020;86:1860–74.
8. Li XJ, Liu C, Zhu XX, Wei HJ, Zhang H, Chen H, et al. Evaluation of tolerability, pharmacokinetics and pharmacodynamics of vicagrel, a novel $P2Y_{12}$ antagonist, in healthy Chinese volunteers. Front Pharmacol. 2018;9:643.
9. Shan JQ, Zhang BY, Zhu YQ, Jiao B, Zheng WY, Qi XW, et al. Overcoming clopidogrel resistance: discovery of vicagrel as a highly potent and orally bioavailable antiplatelet agent. J Med Chem. 2012;55:3342–52.
10. Kazui M, Nishiya Y, Ishizuka T, Hagihara K, Farid NA, Okazaki O, et al. Identification of the human cytochrome P450 enzymes involved in the two oxidative steps in the bioactivation of clopidogrel to its pharmacologically active metabolite. Drug Metab Dispos. 2010;38:92–9.
11. Dansette PM, Rosi J, Bertho G, Mansuy D. Cytochromes P450 catalyze both steps of the major pathway of clopidogrel bioactivation, whereas paraoxonase catalyzes the formation of a minor thiol metabolite isomer. Chem Res Toxicol. 2012;25:348–56.
12. Zhu HJ, Wang XW, Gawronski BE, Brinda BJ, Angiolillo DJ, Markowitz JS. Carboxylesterase 1 as a determinant of clopidogrel metabolism and activation. J Pharmacol Exp Ther. 2013;344:665–72.
13. Guimaraes PO, Tricoci P. Ticagrelor, prasugrel, or clopidogrel in ST-segment elevation myocardial infarction: which one to choose? Expert Opin Pharmacother. 2015;16:1983–95.

14. Xu XY, Zhao X, Yang ZC, Wang H, Meng XJ, Su C, et al. Significant improvement of metabolic characteristics and bioactivities of clopidogrel and analogs by selective deuteration. Molecules 2016;21:704.
15. Qiu ZX, Li N, Song L, Lu Y, Jing J, Parekha HS, et al. Contributions of intestine and plasma to the presystemic bioconversion of vicagrel, an acetate of clopidogrel. Pharmacol Res. 2014;31:238–51.
16. Qiu ZX, Gao WC, Dai Y, Zhou SF, Zhao J, Lu Y, et al. Species comparison of presystemic bioactivation of vicagrel, a new acetate derivative of clopidogrel. Front Pharmacol. 2016;7:366.
17. Jiang JF, Chen XY, Zhong DF. Arylacetamide deacetylase is involved in vicagrel bioactivation in humans. Front Pharmacol. 2017;8:846.
18. Liu C, Zhang YF, Chen WL, Lu YM, Li W, Liu YQ, et al. Pharmacokinetics and pharmacokinetic/pharmacodynamic relationship of vicagrel, a novel thienopyridine $P2Y_{12}$ inhibitor, compared with clopidogrel in healthy Chinese subjects following single oral dosing. Eur J Pharm Sci. 2019;127:151–60.
19. Prakash C, Fan B, Altaf S, Agresta S, Liu H, Yang H. Pharmacokinetics, absorption, metabolism, and excretion of [^{14}C]ivosidenib (AG-120) in healthy male subjects. Cancer Chemother Pharmacol. 2019;83:837–48.
20. Penner N, Xu L, Prakash C. Radiolabeled absorption, distribution, metabolism, and excretion studies in drug development: why, when, and how? Chem Res Toxicol. 2012;25:513–31.
21. Robison TW, Jacobs A. Metabolites in safety testing. Bioanalysis. 2009;1:1193–200.
22. Pusalkar S, Zhou XF, Li YX, Cohen L, Yang JJ, Balani SK, et al. Biotransformation pathways and metabolite profiles of oral [^{14}C]alisertib (MLN8237), an investigational aurora a kinase inhibitor, in patients with advanced solid tumors. Drug Metab Dispos. 2020;48:217–29.
23. Yamada M, Mendell J, Takakusa H, Shimizu T, Ando O. Pharmacokinetics, metabolism, and excretion of [^{14}C]esaxerenone, a novel mineralocorticoid receptor blocker in humans. Drug Metab Dispos. 2019;47:340–9.
24. Lappin G. A historical perspective on radioisotopic tracers in metabolism and biochemistry. Bioanal Graham Lappi. 2015;7:531–40.
25. Murai T, Takakusa H, Nakai D, Kamiyama E, Taira T, Kimura T, et al. Metabolism and disposition of [^{14}C]tivantinib after oral administration to humans, dogs and rats. Xenobiotica 2014;44:996–1008.
26. Meng J, Liu XY, Ma S, Zhang H, Yu SD, Zhang YF, et al. Metabolism and disposition of pyrotinib in healthy male volunteers: covalent binding with human plasma protein. Acta Pharmacol Sin. 2019;40:980–8.
27. Huang M, Wu W, Qian J, Wan DJ, Wei XL, Zhu JH. Body distrubution and in situ evading of phagocytic uptake by macrophages of long-circulating poly (ethylene glycol) cyanoacrylate-co-*n*-hexadecyl cyanoacrylate nanoparticles. Acta Pharmacol Sin. 2005;26:1512–8.
28. Zhang HY, Zhang DL, Ray K, Zhu MS. Mass defect filter technique and its applications to drug metabolite identification by high-resolution mass spectrometry. J Mass Spectrom. 2009;44:999–1016.
29. Zhang HY, Ma L, He K, Zhu MS. An algorithm for thorough background subtraction from high-resolution LC/MS data: application to the detection of troglitazone metabolites in rat plasma, bile, and urine. J Mass Spectrom. 2008;43:1191–200.
30. Bian YC, Zhang H, Ma S, Jiao YY, Yan PK, Liu X, et al. Mass balance, pharmacokinetics and pharmacodynamics of intravenous HSK3486, a novel anaesthetic, administered to healthy subjects. Br J Clin Pharmacol. 2020:1–13. https://doi.org/10.1111/bcp.14363.
31. Hop CECA, Wang Z, Chen Q, Kwei G. Plasma-pooling methods to increase throughput for in vivo pharmacokinetic screening. J Pharm Sci. 1998;87:901–3.
32. Liu C, Lu YM, Sun HB, Yang J, Liu YQ, Lai XJ, et al. Development and validation of a sensitive and rapid UHPLC–MS/MS method for the simultaneous quantification of the common active and inactive metabolites of vicagrel and clopidogrel in human plasma. J Pharm Biomed Anal. 2018;149:394–402.
33. Pereillo JM, Maftouh M, Andrieu A, Uzabiaga MF, Fedeli O, Savi P, et al. Structure and stereochemistry of the active metabolite of clopidogrel. Drug Metab Dispos. 2002;30:1288–95.
34. Bluet G, Blankenstein J, Brohan E, Prévost C, Chevé M, Schofield J, et al. Synthesis of the stabilized active metabolite of clopidogrel. Tetrahedron. 2014;70:3893–900.
35. Gregoire B, Carre MC, Caubere P. Arynic condensation of ketone enolates. New general access to benzocyclobutene derivatives. J Org Chem. 1986;51:1419–27.
36. Park JD, Kim DH. Cysteine derivatives as inhibitors for carboxypeptidase A: synthesis and structure-activity relationships. J Med Chem. 2002;45:911–8.
37. Zhang WC, Shyh-Chang N, Yang H, Rai A, Umashankar S, Ma S, et al. Glycine decarboxylase activity drives non-small cell lung cancer tumor-initiating cells and tumorigenesis. Cell. 2012;148:259–72.
38. Tuffal G, Roy S, Lavisse M, Brasseur D, Schofield J, Touchard ND, et al. An improved method for specific and quantitative determination of the clopidogrel active metabolite isomers in human plasma. Thromb Haemost. 2011;105:696–705.
39. Jia YM, Ge PX, Zhou H, Ji JZ, Tai T, Gu TT, et al. Vicagrel enhances aspirin-induced inhibition of both platelet aggregation and thrombus formation in rodents due to its decreased metabolic inactivation. Biomed Pharmacother. 2019;115:108906.